Comparison of Pt/MWCNTs Nanocatalysts Synthesis Processes for Proton Exchange Membrane Fuel Cells

by

Xuan Liu

A Thesis Presented in Partial Fulfillment
of the Requirements for the Degree
Master of Science in Technology

Approved April 2011 by the
Graduate Supervisory Committee:

Arunachalanadar Madakannan, Chair
Lakshmi Munukutla
Govindasamy Tamizhmani

ARIZONA STATE UNIVERSITY

May 2011

ABSTRACT

Due to the growing concerns on the depletion of petroleum based energy resources and climate change; fuel cell technologies have received much attention in recent years. Proton exchange membrane fuel cell (PEMFCs) features high energy conversion efficiency and nearly zero greenhouse gas emissions, because of its combination of the hydrogen oxidation reaction (HOR) at anode side and oxygen reduction reaction (ORR) at cathode side.

Synthesis of Pt nanoparticles supported on multi walled carbon nanotubes (MWCNTs) possess a highly durable electrochemical surface area (ESA) and show good power output on proton exchange membrane (PEM) fuel cell performance. Platinum on multi-walled carbon nanotubes (MWCNTs) support were synthesized by two different processes to transfer $PtCl_6^{2-}$ from aqueous to organic phase. While the first method of Pt/MWCNTs synthesis involved dodecane thiol (DDT) and octadecane thiol (ODT) as anchoring agent, the second method used ammonium lauryl sulfate (ALS) as the dispersion/anchoring agent. The particle size and distribution of platinum were examined by high-resolution transmission electron microscope (HRTEM). The TEM images showed homogenous distribution and uniform particle size of platinum deposited on the surface of MWCNTs. The single cell fuel cell performance of the Pt/MWCNTs synthesized thiols and ALS based electrode containing 0.2 (anode) and 0.4 mg (cathode) $Pt.cm^{-2}$ were evaluated using Nafion-212 electrolyte with H_2 and O_2 gases at 80 ^oC and ambient pressure. The catalyst synthesis with ALS is relatively simple compared to that with thiols and also showed higher performance (power

density reaches about 1070 $mW.cm^{-2}$). The Electrodes with Pt/MWCNTs nanocatalysts synthesized using ALS were characterized by cyclic voltammetry (CV) for durability evaluation using humidified H_2 and N_2 gases at room temperature (21 ^{o}C) along with commercial Pt/C for comparison. The ESA measured by cyclic voltammetry between 0.15 and 1.2 V showed significant less degradation after 1000 cycles for ALS based Pt/MWCNTs.

To my parents Anping Liu and Shanlian Yu

ACKNOWLEDGMENTS

I would like to express my gratitude to my graduate committee chair as well as my research advisor, Dr. Arunachalanadar Madakannan, who has given me so much useful advices on my research and been patiently guiding me towards the accomplishment of my thesis research. I sincerely thank him for his continuous supports and encouragements during my graduate study.

I am grateful to my thesis committee member, Dr. Lakshmi Munukutla, who has given me so much useful advices on my thesis, for her great supports during my graduate study.

I am thankful to my thesis committee member, Dr. Govindasamy Tamizhmani, for his dedication and commendable guidance throughout my thesis work.

I would like to thank my colleagues and friends, Rashida Villacorta, Anthony Adame, Qurat-ul-ain syed jawed shah, Eric Hinkson, Adam Arvay, Yen Huang, Jiefeng Lin, Chad Mason and Jenchin Yu for their encouragements and inspirations.

I appreciate the assistance from Rene Fischer on the facilities of the projects.

I would like to thank Julie Barnes and Martha Benton for their helps on preparing my graduation.

I thank all my friends for their continuous encouragements.

I acknowledge Arizona State University for providing me an opportunity to pursue my Masters' degree and all the faculty and staff of the Engineering Technology Department for all their assistance during my study at ASU.

Finally, I would like to sincerely thank my parents Anping Liu and Shanlian Yu for their infinite supports in my life.

TABLE OF CONTENTS

Page

CHAPTER Page

LIST OF TABLES

LIST OF FIGURES

Figure Page

CHAPTER 1

INTRODUCTION

1.1 Background

People all around the world are paying more and more attention to the concepts of renewable energy technologies. Compared with traditional fossil fuel based energy technologies, renewable energy is replenished continuously which means it will never run out: there is no shortage of renewable energy as it can be taken from sun, wind, water, plants and garbage to produce electricity and fuel. What is more, renewable energy causes very little damage to the environment. There will be zero or little carbon dioxide emissions to the atmosphere which cause greenhouse effect. Fuel cells are set to be the new power source of the future. What is more, they become one of the most attractive technologies during the past decade due to the fact that the use of fossil fuels for power has resulted in many negative consequences. Some of those include severe pollution, extensive mining of the world's resources, and political control and domination of countries that have extensive resources. As a demand, a new, clean, and renewable power source is needed that is energy efficient, has low pollutant emissions, and can meet the sustainability requirements. Fuel cells are now closer to commercialization than ever, and they have the ability to fulfill all of the global power needs while meeting the efficacy and environmental expectations.

A fuel cell is an electrochemical device that converts chemical energy into electrical energy. Unlike batteries' low energy density due to their volume (see Table 1), fuel cells can continuously generate power from externally supplied

fuels like methanol or hydrogen with oxygen. Theoretically, the fuel cell has the capability of producing electrical energy for as long as possible when there are fuel and oxidant supplied to the electrodes. There are five common types of fuel cell technologies as showed below:

1. Proton Exchange Membrane Fuel Cells (PEMFCs)
2. Alkaline Fuel Cells (AFCs)
3. Phosphoric Acid Fuel Cells (PAFCs)
4. Molten Carbonate Fuel Cells (MCFCs)
5. Solid Oxide Fuel Cells (SOFCs)

Table 1

General fuel cell comparison with other power sources

	Weight	Energy	Volume
Fuel cell	9.5 lb.	2190 Whr	4.0 L
Zinc-air cell	18.5 lb.	2620 Whr	9.0 L
Other battery types	24 lb.	2200 Whr	9.5 L

1.2 Why choose a fuel cell

The use of fossil fuel to produce power has resulted in many negative consequences such as environment pollution, greenhouse effect, and extensive mining of the world's resources. As a result, fuel cell systems have become an attractive power source in recent years. Some advantages of fuel cell systems are as follows [1]:

1. Fuel cells have the potential for a high operating efficiency, scalable to all size power plants.
2. Multiple choices of potential fuel feedstocks, from petroleum products/natural gas to renewable ethanol or biomass H_2 production.
3. Fuel cells have a highly scalable design.
4. If hydrogen is used as a fuel, the only by-product is water.
5. There are no parts, with the exception of pumps, compressors, and blowers to drive fuel and air.
6. Fuel cells can continuously produce power when supplied with fuel.

On the other hand, there are also some limitations common to all fuel cell systems [1]:

1. Fuel cells are currently expensive due to the need for materials with specific properties such as the catalyst material platinum and membrane Nafion based materials. There is a demand to find low-cost replacements or reduce the amount of expensive materials.
2. Fuel reformation technology can be costly and heavy and needs power in order to run.
3. There are durability issues related to fuel cell technologies. The catalyst degradation and electrolyte poisoning must be taken into account.

Compared with conventional power plant, a direct fuel cell power plant has no carnot limitation but high efficiency. It is a clean energy system which

means it emits no pollution into the environment. Furthermore, a fuel cell power plant is quiet and produces no photochemical smog precursor.

1.3 Comparison of fuel cell technologies

Table 2

Comparison of different types of fuel cell systems [2]

Fuel Cell Types	Common Electrolyte	Operating Temperature	System Output	Electrical Efficiency	Combined Efficiency
Polymer Electrolyte Membrane (PEMFC)	Solid organic polymer poly-perfluorosulfonic acid	50-100 ^{o}C	<1kW-250kW	25-58%	70-90%
Alkaline (AFC)	Aqueous solution of potassium hydroxide soaked in a matrix	90-100 ^{o}C	10kw-1MW	60%	>80%
Phosphoric Acid (PAFC)	Liquid phosphoric acid soaked in a matrix	150-200 ^{o}C	50kW-1MW	>40%	>85%
Molten Carbonate (MCFC)	Liquid solution of lithium, sodium	600-700 ^{o}C	<1kW-1MW	45%-47%	>80%
Solid Oxide (SOFC)	Yttria stabilized zirconia	600-1000 ^{o}C	<1kW-3MW	35-43%	<90%

According to Table 2, different types of fuel cells use different types of electrolytes and they work at various temperatures from 50 to 1000 ^{o}C. Higher temperature results higher energy conversion efficiency. The following table shows the applications, as well as the advantages, for each fuel cell technology.

Table 3

Fuel cell applications and advantages [2]

Fuel Cell Types	Applications	Advantages
Polymer Electrolyte Membrane (PEMFC)	1.Backup power 2.Portable power 3.Small distributed generation 4.Transportation 5.Specialty vehicles	1.Solid electrolyte reduces corrosion & electrolyte management problems 2. Low temperature 3. Quick start-up
Alkaline (AFC)	1.Military 2.Space	1.Cathode reaction faster in alkaline electrolyte, leads to higher performance 2.Can use a variety of catalysts
Phosphoric Acid (PAFC)	Distributed generation	1.Higher overall efficiency with CHP 2. Increased tolerance to impurities in hydrogen
Molten Carbonate (MCFC)	1.Electric utility 2. Large distributed generation	1.High efficiency 2.Fuel flexibility 3.Can use a variety of catalysts 3.Suitable for CHP
Solid Oxide (SOFC)	1.Auxiliary power 2. Electric utility 3. Large distributed generation	1.High efficiency 2. Fuel flexibility 3.Can use a variety of catalysts 4.Solid electrolyte reduces electrolyte management problems 5.Suitable for CHP 6.Hybrid/GT cycle

1.4 Scope of work

In my research, I focused on proton exchange membrane fuel cells, so the project is designed to make comparison of Pt/MWCNTs nanocatalysts synthesis processes. Include the following objectives:

1. Synthesizing Pt/MWCNTs nanocatalyst with different length of thiol ligands (Dodecanethiol and Octadecanethiol)
2. Synthesizing Pt/MWCNTs nanocatalyst with ammonium lauryl sulfate as the deposition agent
3. Characterization of Pt/ MWCNTs nanocatalysts by HRTEM, PEMFC test, and durability test

1.5 Organization of the thesis

This thesis involves five chapters: Chapter 1 presents the overall introduction for fuel cells technologies, including the basic background and applications of different kinds of fuel cells; Chapter 2 provides the literature review concerning the PEMFCs and carbon nanotubes technologies; Chapter 3 describes the experimental procedures to prepare Pt/ MWCNTs nanocatalysts; Chapter 4 discusses the results of experiments provided by various tools (HRTEM, PEMFCs stack and cyclic voltammetry tests) to make comparison of Pt/MWCNTs nanocatalysts synthesized by different procedures; Chapter 5 makes the conclusion and provides suggestions for further research in PEMFCs technology.

CHAPTER 2

LITERATURE REVIEW

2.1 Background of PEMFCs

2.1.1 History and applications of PEMFCs

The "father of the fuel cell", Sir William Grove first developed the concept for fuel cells in 1842 [3]. Then in early 1960s, with the work of Tomas Grubb and Leonard Niedrach, General Electric introduced the technology of The PEM fuel cell. This kind of technology was not popular at that time because of its high cost. Not until 20 years later in the late 1980s and early 1990s, was a proof-of- concept fuel cell prototype system developed by Ballard Power Systems (founded in 1979) and thus the applications of PEMFCs have been extended.

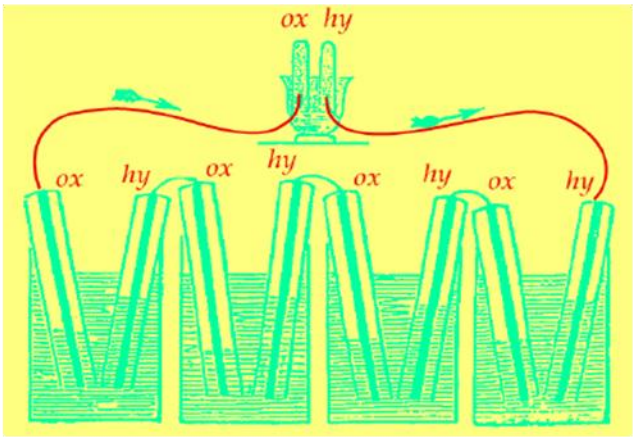

Figure 1 Sir William and the first concept of fuel cell [4]

Proton Exchange Membrane Fuel Cells (PEMFCs) are the most popular type of fuel cell, and traditionally use hydrogen as the fuel. As compared to other types of fuel cells, PEMFCs have relatively lower operational temperature (under 100 ^{o}C), higher power density and efficiency, as well as the ability to respond quickly to transient power. Along with all the distinguishing features, PEMFCs

can also produce power from a fraction of a watt to hundreds of kilowatts which means they can be used in various power applications, from stationary power generation systems through all sizes of mobile devices to vehicles. All these characteristics make PEMFCs particularly attractive for renewable energy technology applications.

A PEMFC consists of a negatively charged electrode (anode), a positively charged electrode (cathode), and an electrolyte membrane. The membrane separate reactants (hydrogen and oxygen/air) from each side but only let protons go through. Hydrogen is oxidized on the anode and oxygen is reduced on the cathode. Protons are transported from anode to cathode, and the electrons reach cathode via external circuit. In nature, molecules cannot stay in an ionic state; therefore they immediately recombine with other molecules in order to return to the neutral state. So oxygen reacts with protons and electrons to form water and release heat. Notice that, the electrochemical processes in both sides need catalyst to speed up. The reactions within a PEM fuel cell are:

$$\text{Anode: } H_2\,(g) \rightarrow 2H^+(aq) + 2e^- \quad (1)$$

$$\text{Cathode: } \tfrac{1}{2}O_2\,(g) + 2H^+\,(aq) + 2e^- \rightarrow H_2O\,(l) \quad (2)$$

$$\text{Overall: } H_2 + \tfrac{1}{2}\,O_2 \rightarrow H_2O\,(l) + \text{Electricity} + \text{Heat} \quad (3)$$

The basic PEM fuel cell stack consists of three components: Channel Plate (bipolar plate), Gas Diffusion Layer (GDL) and Membrane Electrode Assembly (MEA). The MEA is sandwiched with two GDL electrodes on its both sides and the electrochemical reactions are taking place in the interface between MEA and GDLs. The schematic construction of a PEM fuel cell is showed in Figure 2.

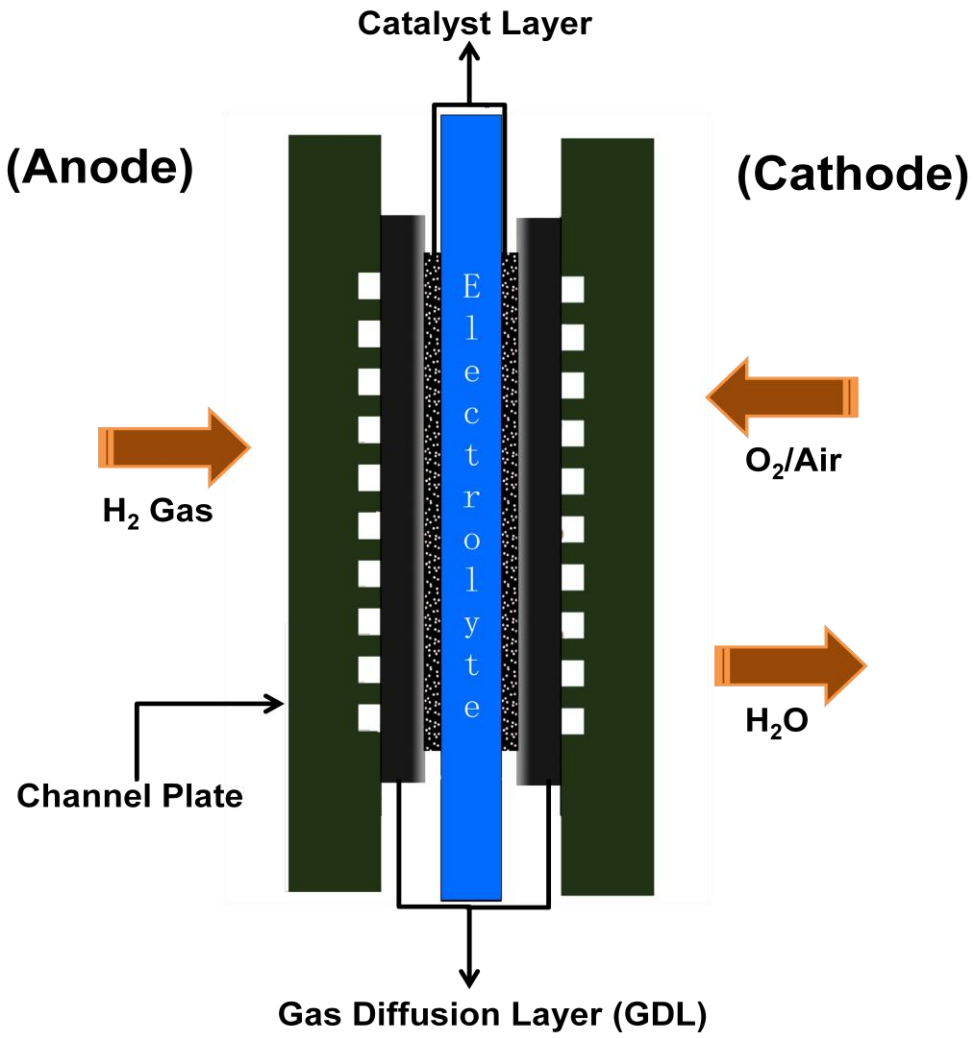

Figure 2 Schematic construction of a PEM fuel cell

Applications of PEM fuel cells can be divided into three categories: transportation, stationary and portable power generation. The power requirement for transportation, such as passenger car, utility vehicles, and bus, ranges from 20 kW to 250 kW. The stationary power requirement has a wide range, from 1 to 50 MW. Then comes to the small scale stationary applications, for example remote telecommunication devices, power requirement is 100W to 1kW. The portable power is usually in the range of 5W to 50W [5].

PEM fuel cells are mainly used for transportation applications because they have little impact to the environment, primarily the control of emission of the green house gases (GHG). Other applications include distributed or stationary, and portable power generation. Due to their high power density and excellent dynamic characteristics as compared with other types of fuel cells, nearly all the automobile companies work solely on PEM fuel cells. In the recent decade, government and researchers are more concerned with sustainable development and realize that the development of PEMFCs plays a significant role for alleviating both the energy crisis and environment issues. Today's companies are being driven by technical, economic, and social forces such as high performance characteristics, reliability, durability, low cost, and environmental benefits.

2.1.2 Basic components of PEMFCs

The three basic components of the PEMFC depicted in Figure 1 are the keys to PEMFCs' performance. To fully understand the fundamental functions of these components in PEMFC system is of great significance in order to optimize the PEMFCs.

1. Channel plate serves as the current collector and fuel flow channel. The pattern of flow field including channel's width and depth can affect the effectiveness of the reactants' distribution and water management.
2. Membrane electrode assembly (MEA) is constructed by the catalyst layer and the electrolyte membrane. Platinum and its alloys are the most effective materials used for PEMFC catalysts also the most

costive component in a PEMFC system. So better distribution of Platinum particles and lower loading can improve the performance and reduce the cost.

3. Gas diffusion layer (GDL). The major functions of GDLs in PEMFCs are: to optimize water management [6], to provide the mechanical support for MEA [7], and act as the electrical contact between the electrodes and the current collectors.

Figure 3 shows the polarization curve of a fuel cell. The ideal voltage is defined by its Nernst potential at the standard conditions (101kPa and 25 ^{o}C). It is 1.229V with liquid water product and 1.18V with gaseous water product [8]. But the actual voltage of a fuel cell is lower than the theoretical result due to three major classifications of losses known as: activation loss, internal resistance loss , and concentration loss. These losses decrease the efficiency of fuel cell and result in loss of useful power output. Also there are other factors affect the performance such as fuel crossover and internal current. The strategy is to minimize these losses. The key components discussed above should be optimized to enhance the performance of fuel cell system.

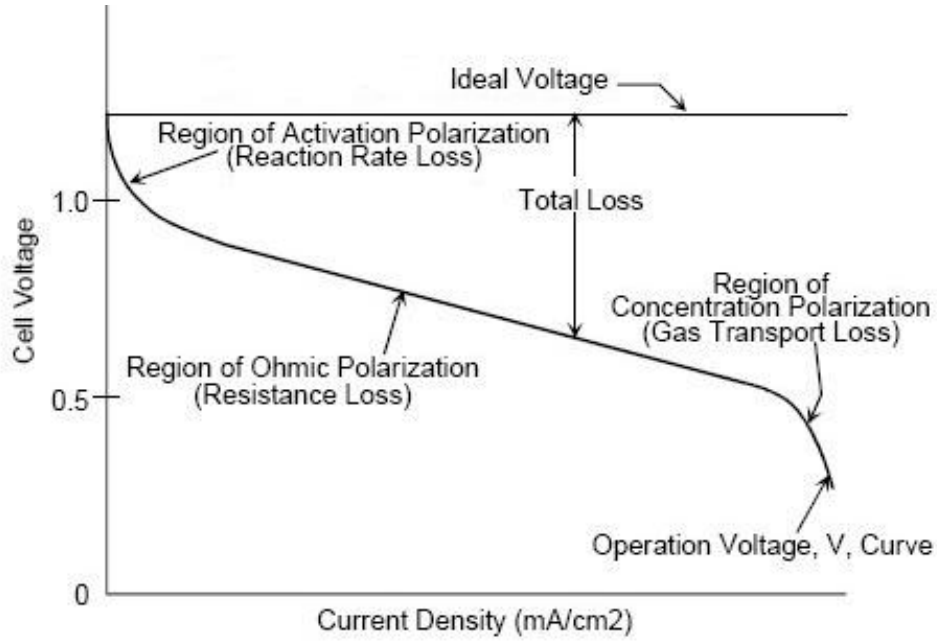

Figure 3 Polarization curve of fuel cell [8]

2.1.3 Technique challenges for PEMFCs applications

The main challenges faced by PEMFCs are: Cost, Performance, and Durability. The cost and durability of PEMFCs are always the major challenges for commercialization of PEMFCs. In addition, system size, weight, thermal and water management in various applications are still the obstacles for PEMFCs. The following technical hurdles have significantly affected the PEMFCs systems according to DOE hydrogen fuel cell program report [9]:

1. Cost: the cost of fuel cell systems is the problem needed to be solved. It is the biggest barrier for fuel cell commercialization. There are several approaches to reduce the cost of fuel cell systems that decreasing the loading of platinum or even finding some other cheaper materials to replace those expensive materials. Also improved fuel cell performance and durability may help to reduce the maintenance cost.

2. Durability and reliability: the goal of fuel cell durability is 5,000 hours lifespan for automotive applications and 40000 hours for stationary applications. What is more, fuel cells should be capable to reliably operate in freeze/thaw conditions. (Starts from indefinite cold-soak at -20℃ and survives from -40℃ for automotive applications and -35 ^{o}C to 40 ^{o}C for stationary applications)
3. System size: the weight and size of fuel cell systems must meet the packaging requirement for automobiles.
4. Air, thermal and water management: the performance of PEMFCs depends on these conditions. A small difference may have a large influence on the fuel cell performance.

To overcome these barriers and achieve commercialization of PEMFC systems, innovations such as new techniques and alternative materials are required. Electrochemical nanoatalyst directly affects the anode and cathode chemical reaction and effectively reflected on the fuel cell performance. Platinum is the most effective electrocatalyst for the PEMFCs because it is sufficiently reactive in bonding hydrogen and oxygen intermediates facilitating the electrode processes to form the final product. But the significantly high cost of Pt in practical PEMFCs limits the catalyst loadings per unit area (or unit power output). The durability of PEMFCs system is typically controlled by the stability of membrane electrode assembly (MEA) includes the characteristics of Pt particles and catalyst support materials.

2.2 Carbon nanotubes as the support material

Carbon is an ideal material for supporting nano-sized metallic particles in the electrode for fuel cell applications. No other material except carbon material has the essential properties of electronic conductivity, corrosion resistance, surface properties, and the low cost required for the commercialization of fuel cells.

2.2.1 Types of carbon nanostructures

Fullerenes or known as buckyballs (see Figure 4) is a molecule with 60 carbon atoms, C_{60}, and with an icosahedral symmetry, or in other words, 60 carbon atoms bonded with each other in 12 pentagons and 20 hexagons. This is the first carbon nanostructure developed by Kroto and his co-workers when they used a pulsed laser beam to evaporate graphite from a rotating disk [10].

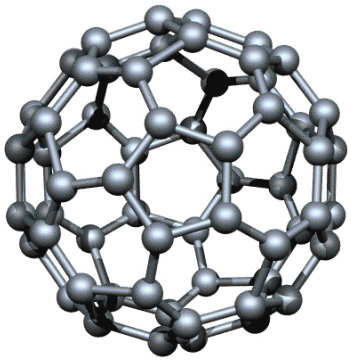

Figure 4 The icosahedral C_{60} molecule [10]

Carbon nanotubes (CNTs) were unexpectedly discovered as a byproduct of fullerenes by direct current (DC) arc discharge; and it becomes today's most promising material in the nanotechnologies. Multi walled carbon nanotubes (MWNTs) was first formed after fullerenes and later single walled carbon nanotubes (SWNTs). SWNTs consist of only single graphene sheet with one

atomic layer in thickness, while MWNTs, as its name, are formed multiple graphene sheets (at least two sheets) arranged concentrically into tube structures. Multi walled carbon nanotubes are formed at relatively lower temperature and at higher temperature the fullerenes forms single walled carbon nanotubes. Both of them are promising one-dimensional periodic structure along the axis of the tube with high aspect ratio (length/diameter).

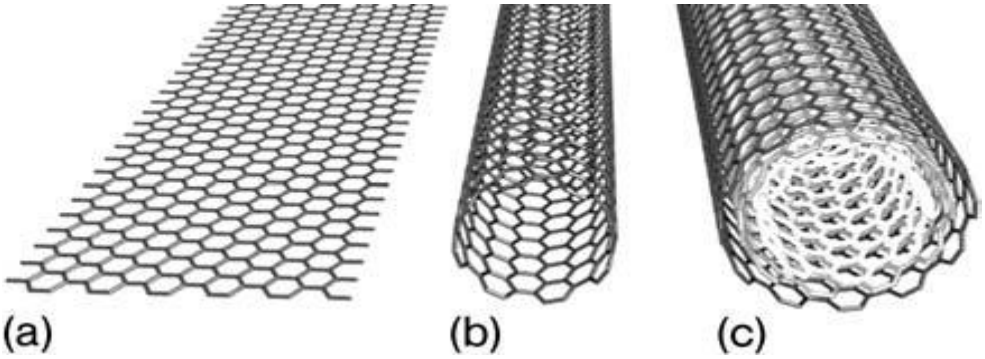

Figure 5 (a) Structure of a single layer of graphite, (b) a single walled carbon nanotube, (c) a multi walled carbon nanotube with three shells [11]

In my thesis, Multi walled carbon nanotubes (MWCNTs) were used as the catalyst support materials, which possess unique characteristics such as:

1. Can be either electrically conductive or semi conductive.
2. High electrical conductivity (same as copper).
3. High thermal conductivity (some as diamond).
4. Superior mechanical strength (100 times greater than steel).

The superior properties of nanotubes make them known as the material of the future. It is ture that new nano and micro applications based on CNTs are identified and proposed every day. Besides fuel cell technology, CNTs are widely

applied in various applications such as nanotechnology, electronics, chemical sensors, also sustainability and energy areas including hydrogen storage.

2.2.2 Synthesis methods of carbon nanostructures

Fullerenes were first synthesized by using an arc discharge method under He atmosphere with high temperature heat treatment. The graphite carbon points were evaporated by the heat generated between electrode, and the graphite concentrate to form soot and fullerenes. The products attached on the water cooled walls of the reactor. Typically this method produces up to 15% fullerenes: C_{60} (~13%) and C_{70} (~2%) in the carbon soot. The fullerenes are abstracted from the soot, by using liquid chromatography and a solvent such as toluene.

Multi walled carbon nanotubes were first discovered by Iijima in the process of producing fullerenes using a plasma arc discharge [12]. Then single walled nanotubes were discovered also when producing endohedral metallo fullerenes using a plasma arc discharge procedure [13, 14]. These novel carbon structures created a new research filed for scientists. After the discovery of CNTs, researchers and scientists grow great interests in the understanding of CNTs' properties as well as the potential applications. Then they tried to develop reliable and efficient methods to achieve commercialization of this attractive structure [15]. The pulsed laser vaporization and the arc discharge methods are first studied because they successfully formed fullerenes and nanotubes. And they helped scientists to get insight into the morphological characteristics properties, and potential applications of CNTs. Then chemical vapor deposition (CVD) was developed and classified as the most reliable method for synthesizing CNTs

because of its potential for scale up production. The three methods discussed above are widely used in the processes of synthesis of carbon nanotubes in current CNTs industry.

For a system to be suitable for the synthesis of carbon nanotubes it must have three essential components:

1. Source of carbon;
2. Source of heat;
3. The presence of metal catalytic particles.

The plasma arc discharge, pulsed laser vaporization (PLV), and chemical vapor deposition (CVD) methods can all, to some extent, provide ideal conditions for CNTs synthesis [15].

2.3 Pt/MWCNTs synthesis methods

The synthesis methods reported in the literature for Pt/CNTs are wet chemical method [16,17], electroless plating [18], electrodeposition [19], self-assembly [20] and supercitrical fluid [21]. However, homogenous deposition of Pt nanoparticles on the inert surface of CNTs is still a challenge in current technology [22]. Surface modification of CNTs with functional groups like -OH, -COOH is commonly carried out by acid oxidation (e.g., HNO_3/H_2SO_4, HNO_3 [23,24], HCl [24], and $KMnO_4$ [25]) with long time sonication at high temperature. On the other hand, extensive acid oxidation processing results in unexpected defects and impurities [26]. Furthermore, according to the research report that CNTs under harsh acidic conditions may break the symmetry of the π-bonding arising from sp^2 hybridization, which is crucial for the adhesion of Pt

nanoparticles on CNTs [27]. According to previous research [20], mild acid, such as citric acid, can provide acid environment and does little damage to CNTs.

CHAPTER 3

EXPERIMENTAL

Platinum on multi-walled carbon nanotubes (MWCNTs) support were synthesized by two different processes to transfer $PtCl_6^{2-}$ from aqueous to organic phase. While the first method of Pt/MWCNTs synthesis involved dodecane thiol (DDT) and octadecane thiol (ODT) as anchoring agent, the second method used ammonium lauryl sulfate (ALS) as the dispersion/anchoring agent.

3.1 Materials

For this project, MWCNTs (OD 20-30 nm) were obtained from Cheaptubes Co., citric acid (CA, $C_6H_8O_7$) and sodium formate (HCOONa) from Spectrum Chemicals, chloroplatinic acid hexahydrate ($H_2PtCl_6.6H_2O$), tetraoctylammonium bromide (ToAB, $N(C_8H_{17})_4Br$), toluene ($C_6H_5CH_3$), 1-dodecanethiol (DDT, $C_{12}H_{25}SH$, 98%), and 1-octadecanethiol (ODT, $C_{18}H_{37}SH$) from Sigma-Aldrich, ammonium lauryl sulfate (ALS) from MP Biomedicals, LLC.

3.2 Synthesizing Pt/MWCNTs nanocatalyst by using thiol ligands

The strategy of synthesizing platinum nanoparticles distributed on MWCNTs is to introduce a thiol ligand for the deposition of Pt nanoparticles which provide homogenous distribution and controlled particle size.

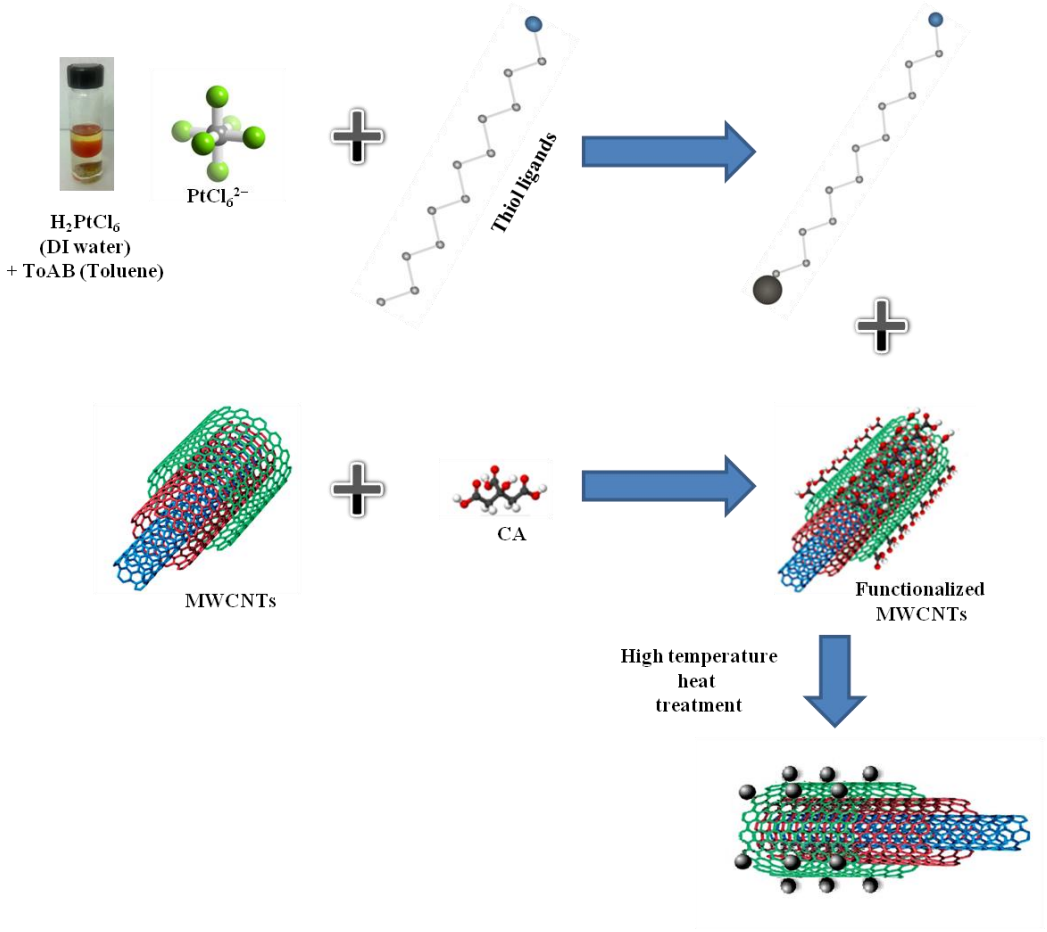

Figure 6 Schematic processes for synthesizing Pt/MWCNTs by using thiol ligands

To prepare Pt/MWCNTs nanocatalyst (thiol ligands), there are three steps:

1. Surface modification of MWCNTs with functionalized groups
2. Stabilize and functionalize $PtCl_6^{2-}$ ions with thiol ligands
3. Deposition of platinum nanoparticles on MWCNTs

3.2.1 Surface modification of MWCNTs

Surface modification of MWCNTs using CA was carried out as follows: 100 mg of MWCNTs and citric acid powder (1.5M) were mixed in 3 cc DI water. Then the solution was subjected to 15 min ultrasonic treatment, followed by a vigorous stirring overnight with a magnetic stirrer at room temperature (21 ^{o}C).

After that, the solvent was removed by filtration and the product was heat treated in air at 250 ^{o}C for 30 min. This treatment improves the wetting characteristics of MWCNTs by create –COOH and –OH functional groups on the surface of MWCNTs. These groups act as anchors for metal deposition. Figure 7 shows the MWCNTs surface before and after modification.

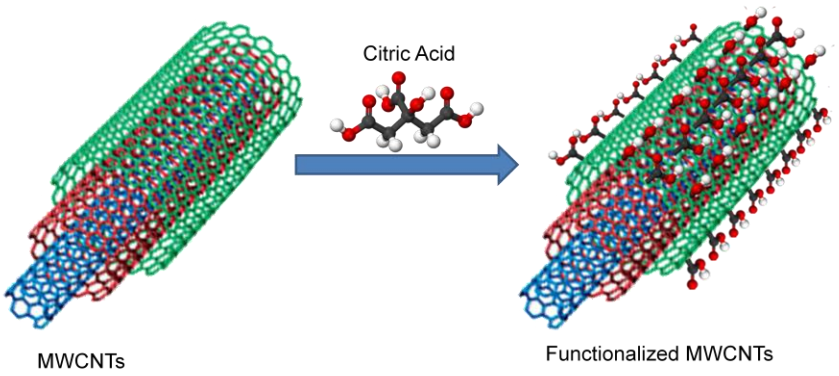

Figure 7 Surface modification of MWCNTs with citric acid [20]

3.2.2 Stabilize and functionalize Pt nanoparticles with thiol ligands

In this process, two-phase (water-toluene) transfer method was introduced to extracts $PtCl_6^{2-}$ ions from aqueous to organic solvent with ToAB. Then thiol ligand was added into the organic solvent and connected with $PtCl_6^{2-}$ ions.

Aqueous chloroplatinic acid (3 cc of 0.04 M in DI water, orange colored) solution was mixed with ToAB solution (3 cc of 0.1 M in toluene, colorless). Then the solution was vigorously stirred for 30 min. The purpose of this process was to abstract $PtCl_6^{2-}$ ions from aqueous solution to organic solution and left H^+ ions by phase-transfer catalyst ToAB. This is evidenced by the observance of the orange

color in the organic layer (top layer), shown in Figure 8. The orange colored organic layer was extracted for next step, then drop-wisely adding thoil ligands (DDT or ODT) into the organic solution and stirred for 30 min. The thiol ligands were self-assembled on the ToAB capturing the $PtCl_6^{2-}$ ions.

Figure 8 Two-phase transfer processes before and after the transfer (thiol ligands based procedure)

3.2.3 Deposition of Pt nanoparticles on MWCNTs

The functionalized MWCNTs were added into the mixture ($PtCl^{2-}$and thiol ligand) prepared above followed by constant stirring for 30 min. then aqueous sodium formate solution (5 cc of 0.3 M) was drop wisely added into the solution and continued stirring for another 30 min at 60 ^{o}C. After that the solvent was removed by using G4 glass frit crucible filter and the solid product was thoroughly rinsed with ethanol to remove the excess thoil ligands. Furthermore, copious amount of warm DI water was used to remove the remaining sodium formate. The final Pt/MWCNTs product was vacuum-dried in furnace at 100 ^{o}C

and further heat treated at 800 ^{o}C for 2 h in a tubular furnace in flowing argon atmosphere.

The whole process chemical reactions are illustrated as following:

$$PtCl_6^{2-}(aq) + N(C_8H_{17})_4^{+}(C_6H_5CH_3) \rightarrow N(C_8H_{17})_4^{+}PtCl_6^{2-}(C_6H_5CH_3) \quad (4)$$

$$mPtCl_6^{2-}(C_6H_5CH_3) + n(\text{thiol ligand})(C_6H_5CH_3) + 4me^{-} \rightarrow$$

$$6mCl^{-}(aq) + (Pt_m)(\text{thiol ligand})_n(C_6H_5CH_3) \quad (5)$$

where the "thiol ligand" presents 1-dodecanethiol (DDT, $C_{12}H_{25}SH$) or 1-octadecanethiol (ODT, $C_{18}H_{37}SH$).

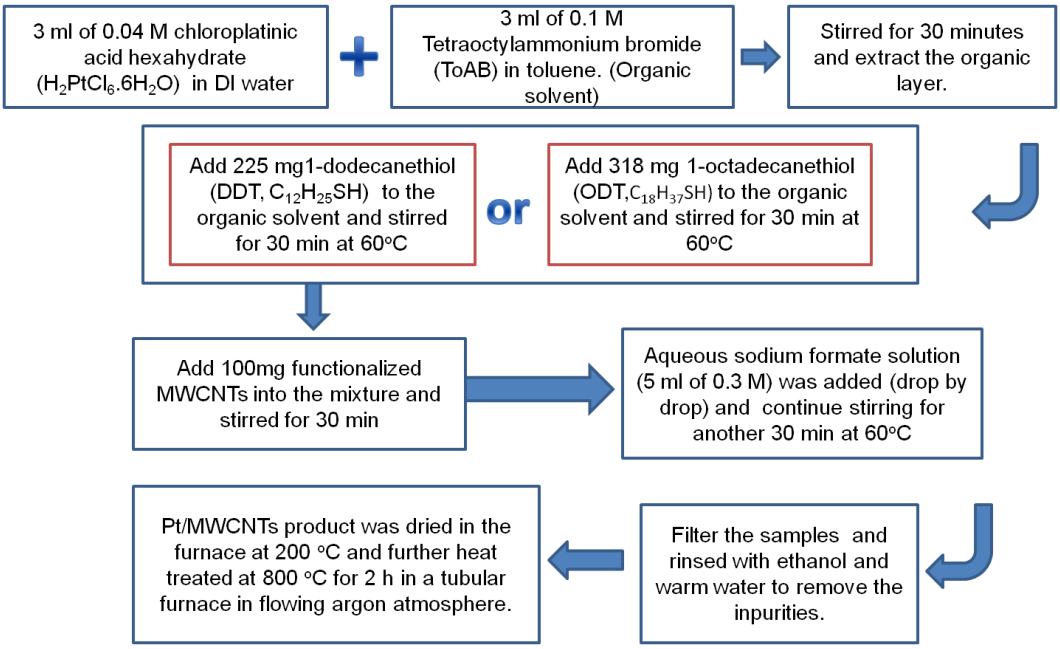

Figure 9 Flow chart of thiol ligands based procedure

The only difference between these two ligands, for this research, is that they have different length of carbon chains. And comparison of the catalyst performance between these two ligands is one of the objects in my thesis.

3.3 Synthesizing Pt/MWCNTs nanocatalyst by using ALS

Ammonium lauryl sulfate (ALS) is also called ammonium dodecyl sulfate ($CH_3(CH_2)_{10}CH_2OSO_3NH_4$). The most significant structure within ALS is a 12-member carbon chain in the molecular backbone. This carbon chain features special function that carbon tail can bond with non-polar portions of molecules and the sulfate head allows ALS to bond with polar molecules such as water.

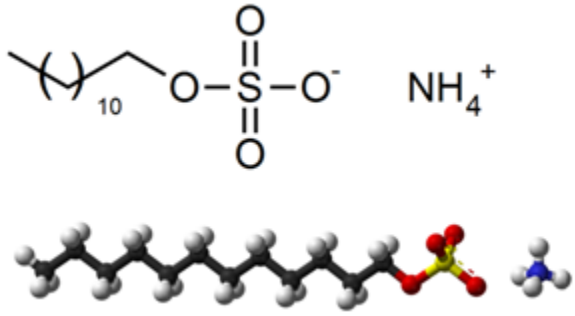

Figure 10 Structure of ALS

The strategy of synthesizing platinum nanoparticles distributed on MWCNTs using ALS is to utilize ALS's feature that it can connect non-polar portions of molecules and polar molecules. In this research, ALS works as a bridge that connect Pt nanoparticle and multi walled carbon nanotubes. This is possible based on the earlier study about the characteristics of ALS [28].

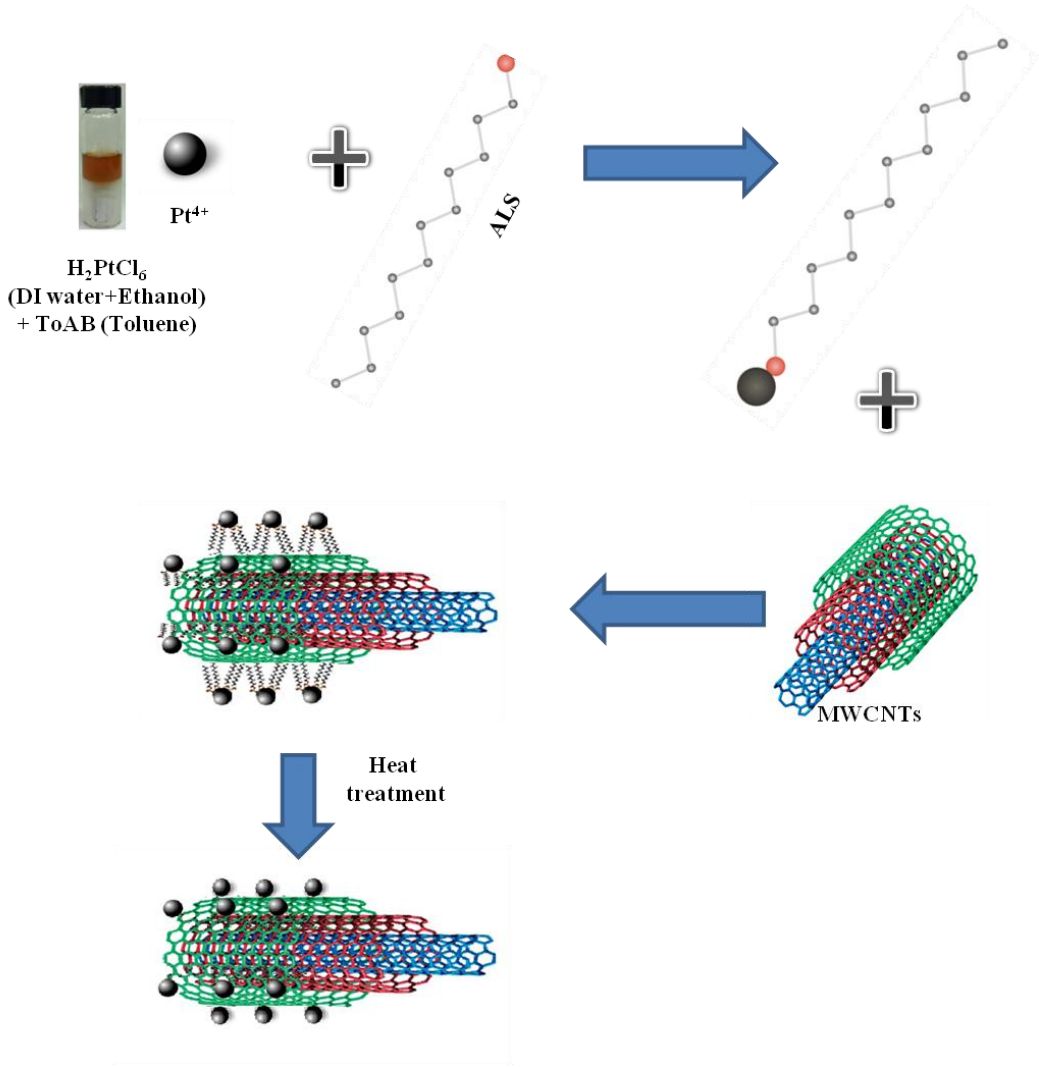

Figure 11 Schematic processes for synthesizing Pt/MWCNTs by using ALS

To prepare Pt/MWCNTs nanocatalyst by using ALS, there are two steps:

1. Stabilize and functionalize platinum ions with ALS
2. Functionalized platinum ions self-assembled on MWCNTs

3.3.1 Stabilize and functionalize Pt ions with ALS

In this process, two-phase (water-toluene) transfer method was introduced to extracts $PtCl_6^{2-}$ ions from aqueous to organic solvent with ToAB. As chloroplatinic acid dissolved in ethanol, the solution with ethanol produced Pt^{4+}

ions instead of $PtCl_6^{2-}$ ions in the organic layer. Then ammonium lauryl sulfate (ALS) was added into the organic solvent and its sulfate head was connected with Pt^{4+} ions.

Aqueous chloroplatinic acid (3 cc of 0.04 M with 1 cc DI water and 2 cc ethanal, orange colored) solution was mixed with ToAB solution (3 cc of 0.1 M in toluene, colorless). Then the solution was vigorously stirred for 30 min. The purpose of this process was to abstract $PtCl_6^{2-}$ ions from aqueous solution to organic solution and left H^+ ions by phase-transfer catalyst ToAB. The difference from the previous procedure was that the $PtCl_6^{2-}$ ions dissolved in ethanol, and divided into Pt^{4+} ions and Cl^- ions in the solvent. As $PtCl_6^{2-}$ molecules transferred, the orange color moved from the aqueous layer (bottom layer) up to the organic layer (top layer). Compared to thiol based synthesis process, the organic layer was highly uniform because of the existence of Pt^{4+} ions, see Figure 12. The aqueous layer was removed and then ALS solution (400 mg in 2 cc ethanol) was drop-wisely added into the orange colored organic solution. After that, the mixture was stirred for 30 min. The negative charged sulfate head of ALS was connected with positive charged Pt^{4+} ions.

Figure 12 Two-phase transfer processes before and after the transfer (ALS based procedure)

3.3.2 Functionalized Pt ions self-assembled on MWCNTs

100 mg MWCNTs were added into the mixture prepared in above step (Pt^{4+} and ALS) followed by constantly stirring for 30 min. Reduction of Pt^{4+} to Pt was carried out using aqueous sodium formate solution (5 cc of 0.3 M) by drop-wise addition at 60 ^{o}C. The reaction product was filtered using G4 glass frit filter and washed thoroughly with warm DI water to remove the remaining sodium formate and ALS. The final Pt/MWCNTs product was vacuum dried at 100 ^{o}C and further heat treated at 200 ^{o}C for 2 h in air.

The whole process chemical reactions are illustrated as following:

$$PtCl_6^{2-}(aq) + N(C_8H_{17})_4^{+}(C_6H_5CH_3) \rightarrow N(C_8H_{17})_4^{+}\,PtCl_6^{2-}(C_6H_5CH_3) \quad (6)$$

$$Pt^{4+} + 4\,CH_3(CH_2)_{10}CH_2OSO_3^{-} \rightarrow (CH_3(CH_2)_{10}CH_2OSO_3)_4Pt \quad (7)$$

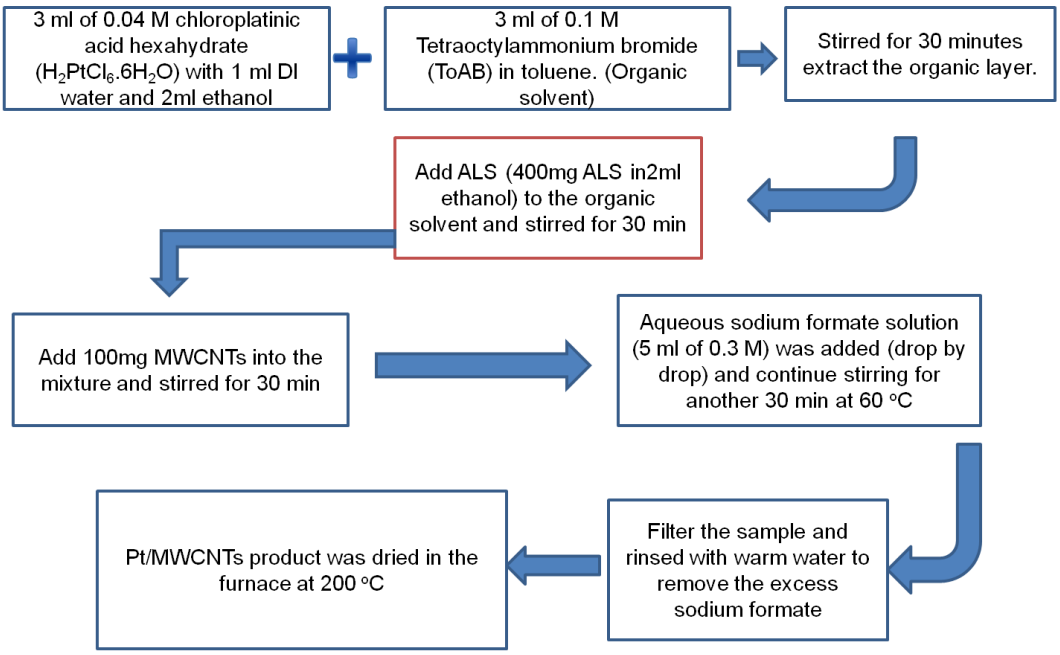

Figure 13 Flow chart of ALS based procedure

3.4 Membrane electrode assembly preparation

Catalyst ink was prepared by adding isopropyl alcohol (25 cc for 1 g of electrocatalyst) and 10 wt % Nafion® (Ion Power Inc., New Castle, DE, USA) dispersion (5 cc for 1 g of electrocatalyst) into Pt/MWCNTs catalyst power purged with flowing argon gas for about 15 minutes. The purge process was done to avoid any flame/ignition of the Pt nanocatalyst particles. The function of Nafion® dispersion was to extend the reaction zone of the catalyst layer as well as create uniform distribution. The catalyst ink was deposited on both sides of Nafion-212 membrane (Ion Power Inc., New Castle, DE, USA) by using micro-spray method to fabricate 5 cm^2 geometrically active areas. The catalyst loadings of the anode and cathode were about 0.2 mg and 0.4 mg Pt per cm^2, respectively. Finally, the catalyst coated membrane (CCM) was vacuum dried at 70 ℃ for 10

min before assembling the MEA in the PEMFC test cell. Commercial Pt/C catalyst (TKK, Japan) based electrodes were also fabricated with similar Pt loading for performance and durability comparison.

3.5 Characterization of Pt/MWCNTs

The MEAs prepared above were assembled by sandwiching inside the single test PEMFC (Fuel Cell Technologies Inc., Albuquerque NM, USA) along with the GDLs on both sides of the CCM. Silicone coated fabric gasket (Product # CF1007, Saint-Gobain Performance Plastics, USA) with a uniform torque of 0.45 kg.m was used to seal the cell. Gaskets were placed between metal plate and membrane on both sides of membrane assembly. The PEMFC single cell was tested in a Greenlight Test Station (G50 Fuel cell system, Hydrogenics, Vancouver, Canada) under following conditions: ambient pressure, 80 ^{o}C, 400 SCCM flow rate of hydrogen for anode and 400 SCCM flow rate of oxygen for cathode.

Durability of the Pt/MWCNTs was evaluated by using potential cyclic voltammetry (CV) of the MEAs by cycling between 0.15 and 1.2 V to accelerate the electrochemically active surface area (ESA) loss of the Pt [29]. In this research, Pt/MWCNTs prepared with ALS and commercial catalyst were operated at ambient temperature with H_2/N_2, 10 mV/s scan rate. The commercial catalyst measured 1000 potential cycles while ALS based catalyst measured 1300 potential cycles using EG&G 2273 PARSTAT potentiostat-galvanostat.

Pt/MWCNTs nanocatalyst dispersed in methanol was applied on a lacy carbon grid for TEM characterization to examine the distribution and particle size of Pt nanoparticles using Philips CM200-FEG.

CHAPTER 4

RESULTS AND DISCUSSIONS

4.1 Comparison of thiol ligands based Pt/MWCNTs nanocatalysts

4.1.1 Performance of DDT and ODT based catalysts in PEMFC

Self-assemble of thiol ligands results physical connection between platinum particles and carbon atoms. Brust *et al* [30] has reported that the unusual property of this thiol-derivatised metal nanoparticle is that they can be handled and characterized as a simple and stable chemical compound. What is more, it produces hydrophobic product with waxy texture on its surface after drying out. However, the thiol ligands would increase the internal resistance of catalyst affecting the overall performance. The solution is to sinter the catalyst powder at high temperature so that the thiol ligands, as well as the function groups on the surface of multi walled carbon nanotubes, can be removed.

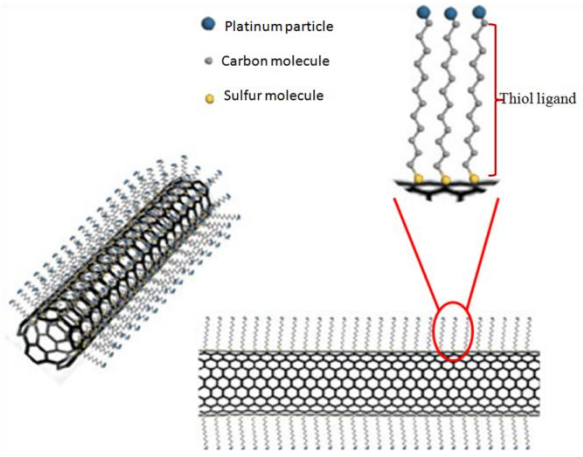

Figure 14 Structure of Pt/MWCNTs synthesized by thiol ligands

As seen in Figure 14 the thiol ligands were added and self-assembled on the surface of ToAB surround $PtCl_6^{2-}$ ions, the carbon tail was connected with

$PtCl_6^{2-}$ ions while sulfate head was attracted by the function group created on MWCNTs.

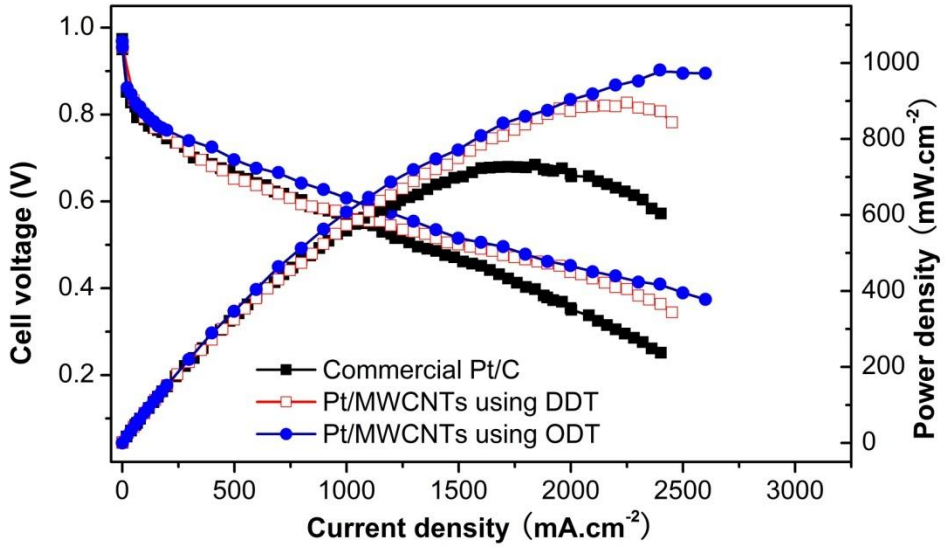

Figure 15 Fuel cell performance of commercial Pt/C catalyst and thiol ligands based Pt/MWCNTs nanocatalysts

Figure 15 shows the single cell performance of Pt/MWCNTs catalysts and commercial Pt/C catalyst. The Pt loadings were 0.2 and 0.4 $mg.cm^{-2}$ at anode and cathode sides, respectively. They were all tested under the same conditions: 80 ^oC, ambient pressure, 100% RH, same GDLs. From the polarization curves, it is obvious that the Pt/MWCNTs catalysts have higher performance than commercial Pt/C catalyst. The peak power density is 727 $mW.cm^{-2}$ for commercial catalyst, 887 $mW.cm^{-2}$ for DDT based catalyst, and 981 $mW.cm^{-2}$ for ODT based catalyst. DDT based catalyst performs almost the same with commercial catalyst at the beginning till around 1000 $mA.cm^{-2}$, then the commercial catalyst voltage drops

quickly while DDT base catalyst performs a relatively flat drop. ODT and DDT have the same molecule structure except that ODT has a longer carbon chain than DDT. It is easy to see that ODT based catalyst performs better than DDT based catalyst. As seen from the figure, ODT based catalyst owned flatter polarization curve, both the activation losses and internal resistance losses are less than DDT based catalyst. In the thiol procedure, longer length of carbon chains gives higher performance.

4.1.2 TEM results of DDT and ODT based Pt/MWCNTs catalysts

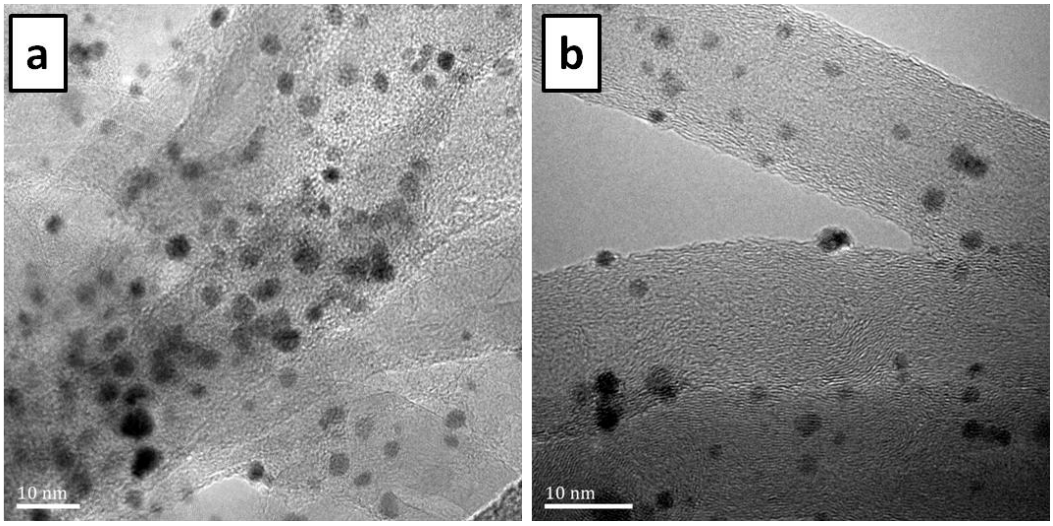

Figure 16 TEM images of Pt/MWCNTs catalyst prepared with: (a) DDT, (b) ODT

Figure 16 (a) and (b) show the high resolution TEM images of Pt/MWCNTs nanocatalysts synthesized using DDT and ODT, respectively. As seen from the TEM images, the Pt nanoparticles are distributed homogenously on the surface of MWCNTs. It is evident from the TEM image in Figure. 16(b) that the Pt particles on the MWCNTs synthesized using ODT is relatively smaller without any agglomeration compared to that using DDT (Figure 16 (a)).

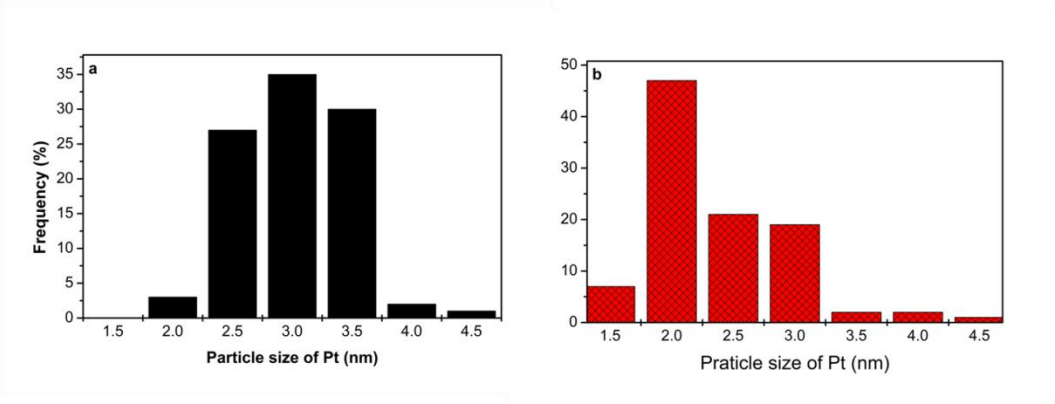

Figure 17 Distributions of Pt particle size: (a) DDT based Pt/MWCNTs and (b) ODT based Pt/MWCNTs

Figure 17 compares the particle size distribution of Pt for the Pt/MWCNTs synthesized using DDT, ODT. The data indicates that the Pt particle size (mean) for DDT and ODT based catalysts is around 3 and 2.3 nm, respectively. As seen from the histograms, ODT based synthesis led to narrow distribution of Pt particles compared to that with DDT. The result shows that the catalyst prepared with longer carbon chain offers smaller and more uniform distributed Pt particles.

4.2 Comparison of different Pt/MWCNTs synthesis procedures

As discussed before, different length of thiol ligands performs differently. In this section, nanocatalyst prepared by using ALS as the deposition agent is taken into comparison.

4.2.1 Performance of different Pt/MWCNTs synthesis procedures

Figure 18 shows the performance comparison of Pt/MWCNTs catalyst prepared by different procedures. All the samples were tested under the same conditions: The Pt loadings were 0.2 and 0.4 mg.cm^{-2} at anode and cathode sides, respectively. Using H_2/O_2 gases, 80 ^{o}C, ambient pressure, 100% RH, same GDLs

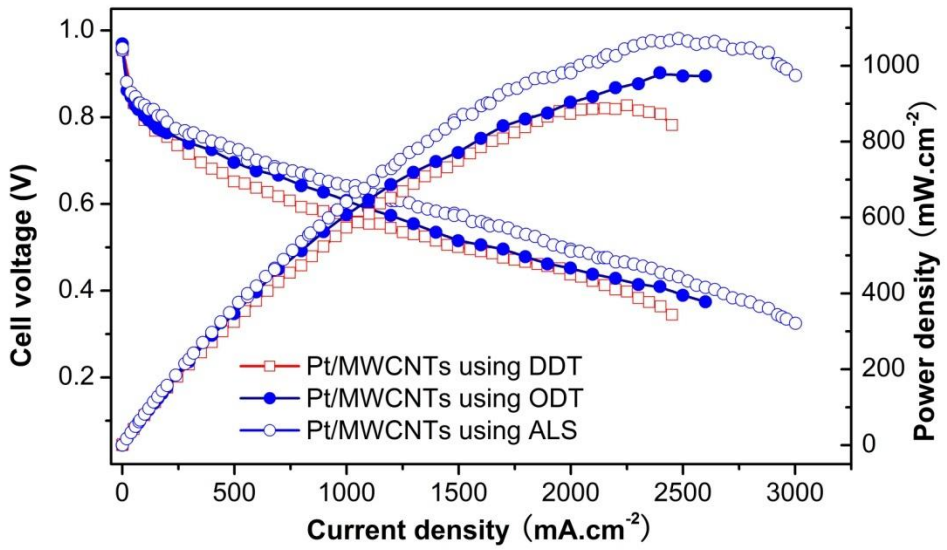

Figure 18 Performance of Pt/MWCNTs nanocatalysts prepared by different procedures

As shown in Figure 18, ALS based catalyst features highest peak power density (1070 $mW.cm^{-2}$). Though lower open circuit voltage, ALS based catalyst suffers less activation and internal resistance lost. The polarization curve of ALS based catalyst always maintains higher level among all the samples. Between two Pt/MWCNTs synthesis procedures, ALS based process works better than thiol based procedure.

4.2.2 TEM results of different Pt/MWCNTs synthesis procedures

To make the comparison of different procedures, TEM images of DDT and ODT are put together with ALS.

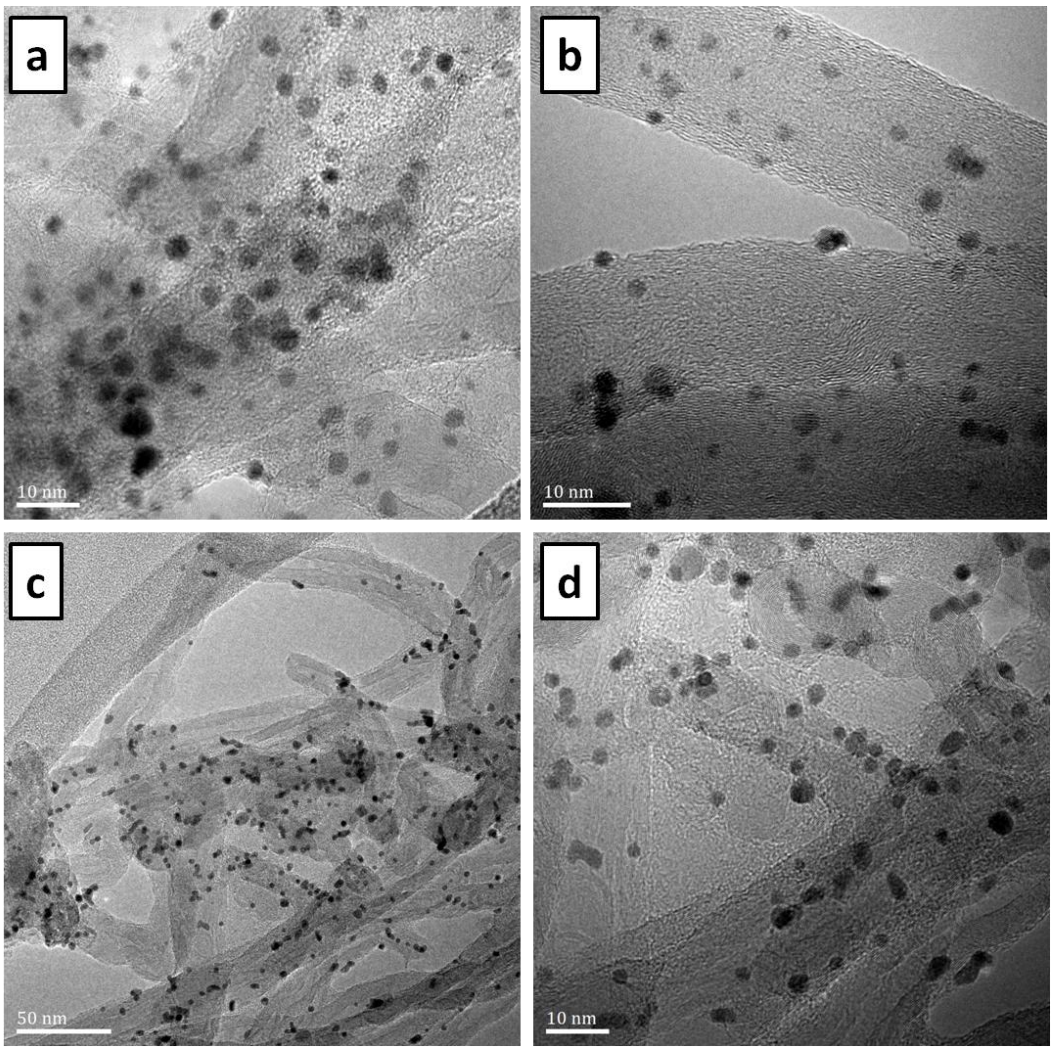

Figure 19 TEM images of (a) DDT, (b) ODT, and (c), (d) ALS

Pt/MWCNTs nanocatalyst synthesized using ALS are shown in Figure 19 (c) and (d) at two different magnifications. From the TEM images, the Pt nanoparticles were homogenous deposited on the surface of multi walled carbon nanotubes. And compared with thiol based catalysts, ALS based nanocatalyst features uniform distribution of Pt particles and narrow range of particle size.

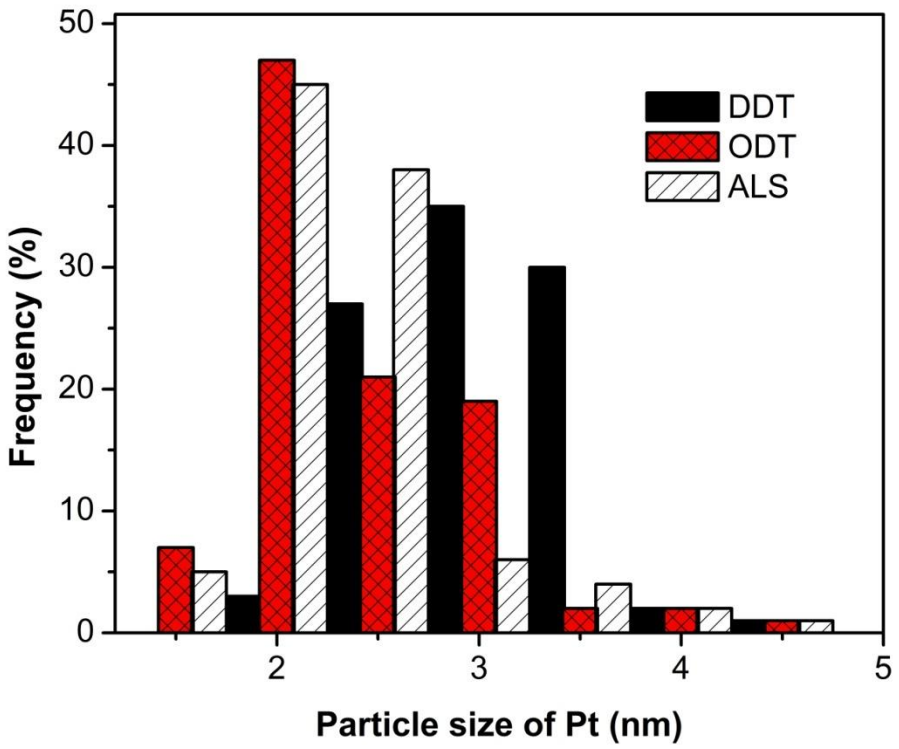

Figure 20 Particle size distributions of Pt/MWCNTs synthesized using (a) DDT, (b) ODT and (c) ALS

Figure 20 compares the particle size distribution of Pt for the Pt/MWCNTs synthesized using different procedures. The result of thiol based catalyst has been discussed in previous sections. In this section, Pt distribution of ALS based catalyst is taken into comparison. As seen from the histograms, the Pt particle size (mean) is about 2.2 nm (almost similar to the ODT based catalyst) for the ALS based catalyst. However, unlike the ODT based Pt/MWCNTs catalyst, the particles are distributed within a narrow range of 2-2.5 nm with more uniform Pt particles than thiol ligands based Pt/MWCNTs catalysts.

4.2.3 Differences between two Pt/MWCNTs synthesis procedures

According to the above comparisons of different procedures, obviously, ALS based catalyst are better than thiol ligands based catalyst. Though they have similar preparation processes, they work in different principles.

To begin with, in thiol ligands procedure, two-phase transfer method was processed with water and toluene. The hexachloroplatinic acid could not dissolved in toluene and was surrounded by ToAB, see Figure 21 (a). Then thiol ligands were added and self-assemble on the surface of $PtCl_6^{2-}$ ions, the carbon tail was connected with $PtCl_6^{2-}$ while sulfate head was attracted by the function groups created on MWCNTs, see Figure 22. On the other hand, in the ALS procedure, two-phase transfer method was carried with water, ethanol, and toluene. The hexachloroplatinic acid dissolved in ethanol and appeared as Pt4+ ions in the organic layer which showed uniform solvent, see Figure 21 (b). After that, ALS was added, the negative charged sulfate head was attracted by the positive charged Pt^{4+} ions while the carbon tail self-assembled on the surface of MWCNTs, see Figure 22.

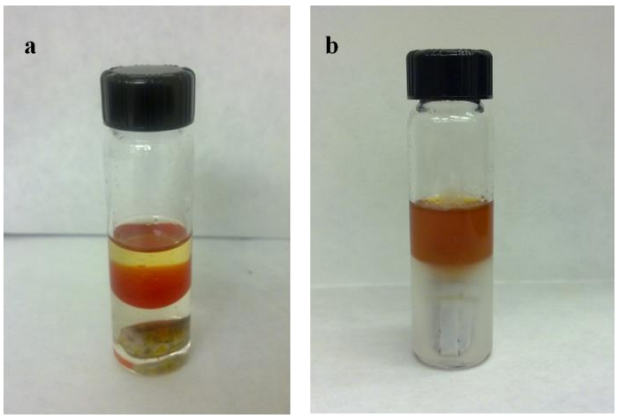

Figure 21 Two-phase transfer process: (a) thiol procedure and (b) ALS procedure

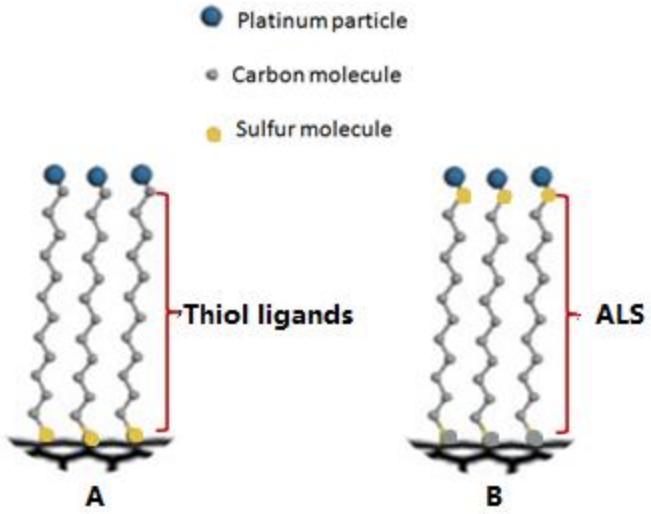

Figure 22 Difference between thiol and ALS procedures

What is more, the thiol ligands based catalyst needs to be sintered at 800 ^{o}C in flowing argon atmosphere to remove the impurities. ALS based catalyst, however does not need such process because the boiling point of ALS is around 200 ^{o}C and there are no function groups on the surface of MWCNTs. The function groups created by citric acid work as anchors for deposition of platinum particles in thiol ligands procedure, but in ALS procedure, the carbon chains are self-assembled onto the surface of carbon nanotubes. Compared to thiol ligands procedure, ALS procedure produce higher performance nanocatalyst and is much more cost-effective because of the reduced steps and materials due to elimination of functionalization with CA.

4.3 Durability tests of ALS based catalyst and commercial catalysts

The cyclic voltammetry tests were carried out using humidified H_2/N_2 gases in the voltage range of 0.15 to 1.2 V with 10 $mV.s^{-1}$ scan rate at 25 ^{o}C for 1000 cycles for both the Pt/C and Pt/MWCNTs based MEAs. The ESA values

were calculated from the CV data using the hydrogen desorption area (between 0.15 and 0.4 V) by assuming a charge of 210 210 $\mu C.cm^{-2}$ for the electroactive Pt surface. Then, the specific ESA was calculated based on the following relation:

$$\text{Specific ESA} = Q_h/(m*q_h) \quad (8)$$

where Q_h is the charge for hydrogen desorption, m is the Pt metal loading, and q_h is the charge required for desorbing a monolayer of hydrogen on Pt surface [31]. ESA data are given in Table 4.

Table 4

Durability test data of commercial Pt/C catalyst and ALS based Pt/MWCNTs catalyst

	ESA values ($m^2.g^{-1}$ of Pt) at various cycles						Peak power density ($mW.cm^{-2}$)	
	1^{st}	100^{th}	300^{th}	500^{th}	700^{th}	1000^{th}	Before CV	After CV
Pt/C	70	63.2	63	61	58	56	730	430
Pt/MWCNTs	76	75.6	75.2	74.6	74	70	1070	915

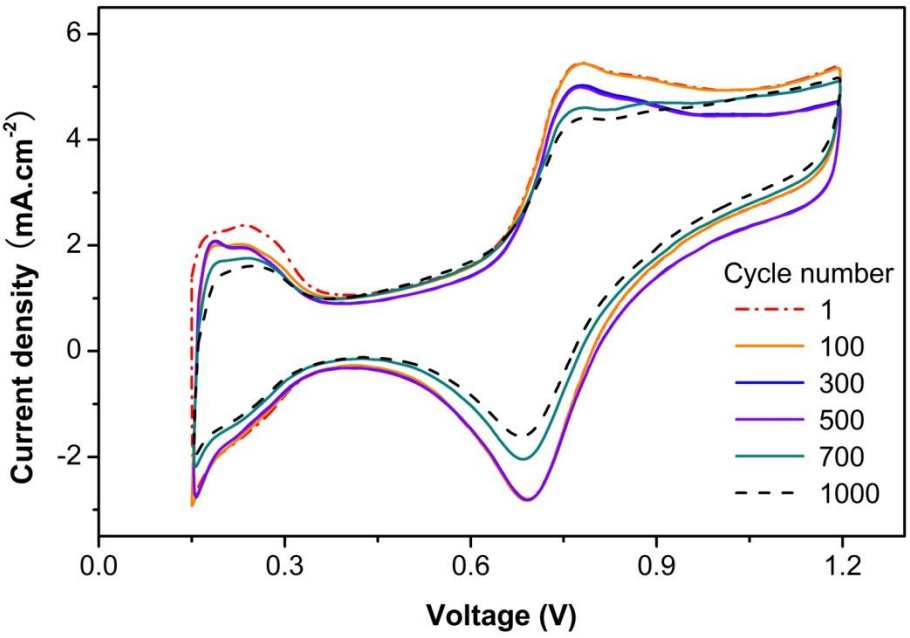

Figure 23 Cyclic voltammetry data for MEAs with commercial Pt/C for 1st, 100th, 300th, 500th, 700th and 1000th cycles

Figure 23 compares the CV curves for commercial Pt/C catalyst based MEA at the 1st, 100th, 300th, 500th, 700th and 1000th cycles. As evident from the Figure 23, the CV profiles changed significantly as the cycle numbers increased showing lower hydrogen desorption area. As seen from the Table 4, the ESA values decreased (by 20 %) from 70 at the 1st cycle to 56 $m^2.g^{-1}$ at the 1000th cycle. It suffers a quick drop at 100th cycle and maintains till the 500th cycle, the ESA value for this period is around 62 $m^2.g^{-1}$. After that, the ESA keep decreasing from 58 $m^2.g^{-1}$ at 700th cycle to 56 $m^2.g^{-1}$ at 1000th cycle.

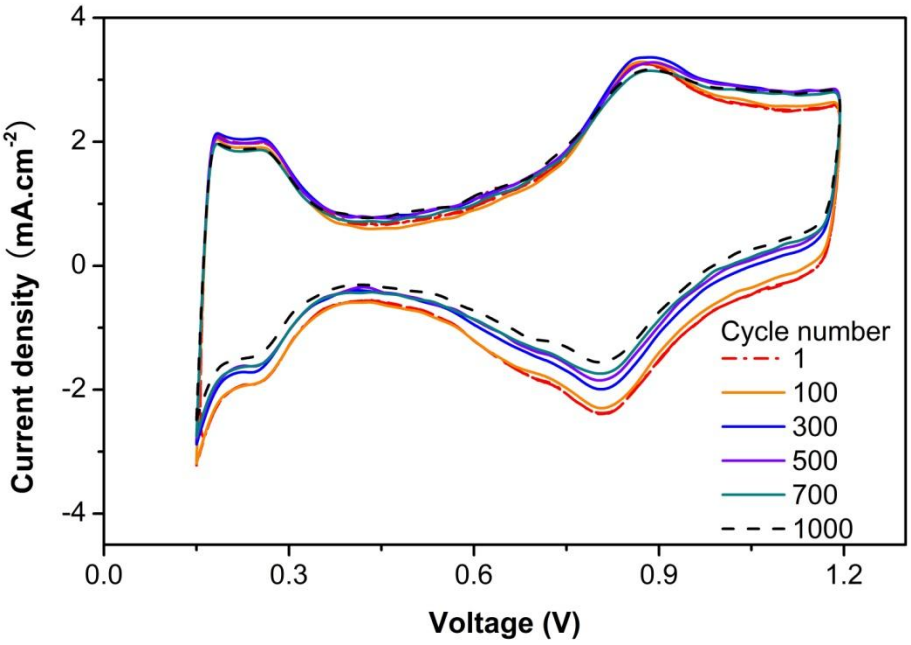

Figure 24 Cyclic voltammetry data for MEAs with Pt/MWCNTs synthesized using ALS for 1st, 100th, 300th, 500th, 700th and 1000th cycles

Figure 24 shows the CV curve of ALS based catalyst, ESA values were also calculated from CV data. Unlike the curve of commercial catalyst, ALS based catalyst possesses higher electrochemical surface area (ESA) (range from 0.15-0.4V). From the first cycle to 700th cycle, the ESA remains almost unchanged, as shown in Table 4 the ESA value for this period is 76 $m^2.g^{-1}$. Then at 700th cycle, the ESA decreases to 74 $m^2.g^{-1}$. Then keep shrinking to 70 $m^2.g^{-1}$at 1000th cycle. The total ESA lose for ALS based catalyst is 8% after 1000 cycles CV test.

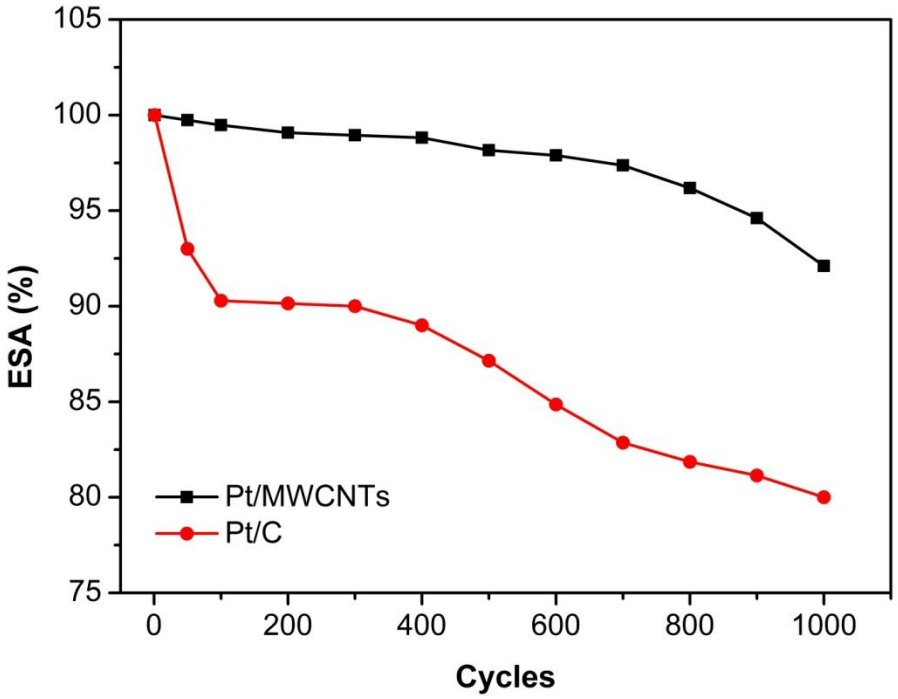

Figure 25 ESA percentage losses during CV test

Figure 25 shows the ESA percentage losses of Pt/C and Pt/MWCNTs catalysts. Based on the potential cycling data, it is evident that the Pt/MWCNTs nanocatalyst synthesized using ALS is highly stable compared to the commercial Pt/C catalyst.

Polarization curves before and after CV test were taken for comparison. Figure 26 presents the performance of commercial Pt/C catalyst and ALS based Pt/MWCNTs catalyst.

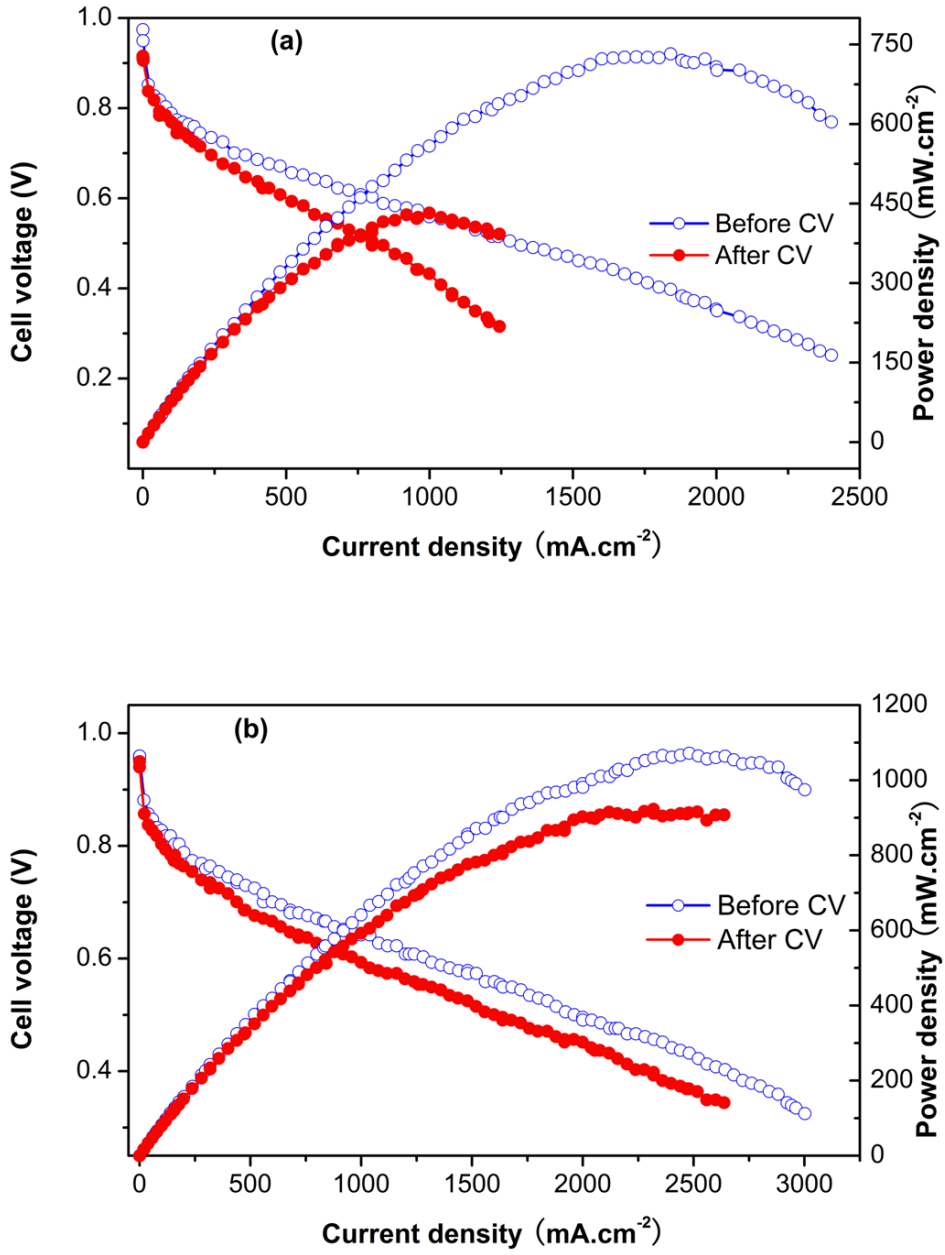

Figure 26 Performance of: (a) commercial Pt/C catalyst and (b) ALS based Pt/MWCNTs catalyst before and after CV test

The performance of commercial catalyst (see Figure 26 (a)) is dramatically decreased. The peak power density drops from 730 to 430 $mW.cm^{-2}$

after 1000 cycles CV test. The open circuit voltage also drops. About 40 % of commercial catalyst performance was lost during the durability test. On the other hand, Figure 26 (b) shows the polarization curves of ALS based catalyst before and after CV test. Before test, the peak power density of ALS based catalyst was 1070 $mW.cm^{-2}$. Even after 1000 cycles CV test, the peak power density decreased to 915 $mW.cm^{-2}$. Hence the overall performance loss of ALS based Pt/MWCNTs catalyst is only < 15 %.

Nanoparticles inherently show a strong tendency to agglomerate due to their high specific activity or surface area [32,33]. When platinum particles agglomerate to bigger particles, the electrochemical surface area decreases, and results in performance degradation. Both ESA values and polarization curve present that ALS based catalyst is more durable and stable than commercial catalyst. As discussed above, commercial catalyst lost 40 % performance after 1000 cycles accelerated durability test while ALS based catalyst only lost 15 % performance after 1000 cycles accelerated durability test.

CHAPTER 5

CONCLUSIONS

The Pt/MWCNTs nanocatalysts were synthesized by the two-phase transfer of Pt complex followed by sodium formate reduction in presence of DDT, ODT and ALS. The surface modification/functionalization of MWCNTs using citric acid process was eliminated for the ALS based Pt/MWCNTs synthesis, shortening the process steps. The synthesis process using ALS has the advantages of decreasing the size of catalyst while increasing the fuel cell performance and stability of the MEA. High-resolution TEM analysis revealed that a highly homogenous dispersion of Pt nanoparticles with a size range of 2-2.5 nm was deposited on the non-functionalized MWCNTs in the ALS based synthesis process. The single cell PEMFC with a total catalyst loading of 0.6 mg $Pt.cm^{-2}$ (anode: 0.2 mg $Pt.cm^{-2}$ and cathode: 0.4 mg $Pt.cm^{-2}$) exhibited a peak high power density of 1070 $mW.cm^{-2}$ using H_2/O_2 at 80 ℃ and ambient pressure. High durability and stability of the Pt/MWCNTs synthesized using ALS based process were indicated by the stable ESAs and peak power density values before and after 1000 CV cycles testing compared to the commercial Pt/C catalyst.

Synthesis of Pt nanoparticle supported on multi walled carbon nanotubes (MWCNTs) possess higher electrochemical surface area (ESA) and show good power output on proton exchange membrane (PEM) fuel cell performance. However, the electrochemical stability of membrane electrode assembly (MEA) with Pt/MWCNTs nanocatalysts are still unable to reach the current goal of department of energy (DOE, the target of stability for fuel cells is 5000 hours for

automobile applications and 40000 hours for stationary applications). In further researches, TiO_2 nanoparticles can be introduced to form a thin buffer layer for the attachment of Pt nanoparticles which provide highly electrochemical durability and reduced material cost.

REFERENCES

[1]. Spiegel, C. (2008). *PEM Fuel Cell Modeling and Simulation Using MATLAB.* Elsevier Inc.

[2]. Comparison of Fuel Cell Technologies. U.S. Department of Energy Hydrogen Program. http://www1.eere.energy.gov/hydrogenandfuelcells/fuelcells/pdfs/fc_comparison_chart.pdf

[3]. J. Zhang. *PEM Fuel Cell Electrocatalysts and Catalyst Layers: Fundamentals and Applications.* Springer-Verlag London Ltd, Gulldford, Surrey,U.K, 2008

[4]. U.S. Department of Energy. Energy efficiency and renewable energy. http://www1.eere.energy.gov/vehiclesandfuels/pdfs/deer_2004/session1/2004_deer_fairbanks.pdf

[5]. Lipman T, Sperling D. Market concepts, competing technologies and cost challenges for automotive and stationary applications. In: Vielstich W, Gasteiger H, Lamm A, editors. *Handbook of fuel cells: fundamentals, technology and applications.* John Wiley & Sons, Ltd.; 2003. p. 1318–28

[6]. U.S. Department of Energy Hydrogen Program. March 2009. http://www1.eere.energy.gov/hydrogenandfuelcells/pdfs/doe_h2_program.pdf

[7]. S. Thomas, M. Zalbowitz, Jim Cruz. *Fuel Cells - Green Power*. Los Alamos National Laboratory. 1999

[8]. C.S. Kong, D.Y. Kim, H.K. Lee, Y.G. Shul, T.H. Lee. Influence of pore-size distribution of diffusion layer on mass-transport problems of proton exchange membrane fuel cells. *J. Power Sources,* 108, (2002): 185-191

[9]. U.S. Department of Energy Hydrogen Program, March 2009, http://www1.eere.energy.gov/hydrogenandfuelcells/fuelcells/fc_challenges.html

[10]. Kroto HW, Heath JR, O'Brien SC, Curl RF, Smalley RE. C60: buckminsterfullerene. *Nature*, 1985; 318:162-3

[11]. V. Kamavaram, V. Veedu and A.M. Kannan. Synthesis and characterization of platinum nanoparticles on in situ grown carbon nanotubes based carbon paper for proton exchange membrane fuel cell cathode. *J. Power Sources,* 188 (2009): 51-56

[12]. Iijima S. Helical microtubules of graphitic carbon. *Nature,* 1991; 354:56-8

[13]. Iijima S, Ichihashi T. Single-shell carbon nanotube of 1-nm diameter. *Nature*, 1993; 363:605-5

[14]. Bethune DS, Kiang CH, Vries MS, Gorman G, Savoy R, Vazquez J, et al. Cobalt-catalyzed growth of carbon nanotubes with single-atomic-layer walls. *Nature,* 1993; 363:605-7

[15]. Wilson Merchan-Merchana, Alexei V. Savelievb, Lawrence Kennedyc, Walmy Cuello Jimeneza. Combustion synthesis of carbon nanotubes and related nanostructures. *Energy and Combustion Science*, 36 (2010) 696-727

[16]. S. Banerjee, S.S. Wong. In situ quantum dot growth on multi-walled carbon nanotubes. *J. Am. Chem. Soc.*, 125 (2003) 10342-10350

[17]. X.R. Ye, Y.H. Lin, C.M. Wang, C.M. Wai. Synthesis of carbon nanotubes with totally hollow channels and/or with totally copper filled nanowires. *Adv. Mater.*, 15 (2003) 316-319

[18]. Z.L. Liu, X.H. Lin, J.Y. Lee, W. Zhang, M. Han, L.M. Gan. Preparation and characterization of platinum-based electrocatalysts on multiwalled carbon nanotubes for proton exchange membrane fuel cells. *Langmuir*, 18 (2002) 4054-4060

[19]. Q. Xu, L. Zhang, J. Zhu. Controlled growth of composite nanowires based on coating Ni on carbon nanotubes by electrochemical deposition method. *J. Phys, Chem.,* 107B (2003) 8294-8296

[20]. J.F. Lin, V. Kamavaram, A.M. Kannan. Synthesis and characterization of carbon nanotubes supported platinum nanocatalyst for proton exchange membrane fuel cells. *J. Power Sources*, 195 (2010) 466-470

[21]. A.D. Taylor, R.C. Sekol, J.M. Kizuka, S.D. Cunha, C.M. Comisar. Fuel cell performance and characterization of 1-D carbon-supported platinum nanocomposites synthesized in supercritical fluids. *J. Catalysis*, 259 (2008) 5-16

[22]. K. Lee, J.J. Zhang, H.J. Wang, D.P. Wilkinson. Progress in the synthesis of carbon nanotube- and nanofiber-supported Pt electrocatalysts for PEM fuel cell catalysis. *J. Appl. Electrochem.,* 36 (2006) 507-522

[23]. T. Kyotani, S. Nakazaki, W.H. Xu, A. Tomita. Chemical modification of the inner walls of carbon nanotubes by HNO oxidation. *Carbon*, 39 (2001) 771-785

[24]. A.G. Osorio, I.C.L. Silveira, V.L. Bueno, C.P. Bergmann. H2SO4/HNO3/HCl-Functionalization and its effect on dispersion of carbon nanotubes in aqueous media. *Appl. Surface Sci.*, 255 (2008) 2485-2489

[25]. V. Hacker, E. Wallnofer, W. Baumgartner, T. Schaffer, J.O. Besenhard, H. Schrottner, M. Schmied. Carbon nanofiber-based active layers for fuel cell cathodes – preparation and characterization. *Electrochem. Comm.*, 7 (2005) 377-382

[26]. M. Monthioux , B.W. Smith , B. Burteaux , A. Claye , J.E. Fischer , D.E. Luzzi. Sensitivity of single-wall carbon nanotubes to chemical processing: an electron microscopy investigation. *Carbon*, 39 (2001) 1251–1272

[27]. C. Richard, F. Balavoine, P. Schultz, T.W. Ebbesen, C. Mioskowski. Supramolecular self-assembly of lipid derivatives on carbon nanotubes. *Science*, 300 (2003) 775-778

[28]. S.Jansson, R. Modin, G. Schill. Two-phase titration of organic ammonium ions with lauryl sulphate and methyl yellow as indicator. *Talanta*, 21(1974) 905-918

[29]. X. Yuan, H. Wang, J.C. Sun, J. Zhang, AC impedance technique in PEM fuel cell diagnosis – A review. *Int. J. Hydrogen Energy* 32 (2007) 4365-4380

[30]. M. Brust, M. Walker, D. Bethell, D.J. Schiffrin and R. Whyman. Synthesis of thiol-derivatised gold nanoparticles in a two-phase liquid-liquid system. *J. Chem. Soc., Chem*. Comm., (1994) 801-802

[31]. Sheng-Yang Huang, Prabhu Ganesan, Branko N. Popov. Titania supported platinum catalyst with high electrocatalytic activity and stability for polymer electrolyte membrane fuel cell. *Applied Catalysis B: Environmental* 102 (2011) 71–77

[32]. J. Xie, D.L. Wood, K.L. More, P. Atanassov, R.L. Borup. Microstructural changes of membrane electrode assemblies during PEFC durability testing at high humidity conditions. *J. Electrochem. Soc*. 152 (2005) A1011-1020

[33]. E. Guilminot, A. Corcella, F. Maillard, M. Chatenet. Detection of Pt^{z+} ions and Pt nanoparticles inside the membrane of a used PEMFC. *J. Electrochem. Soc*., 154 (2007) B96-B105